Atmospheric Research 104-105 (2012) 292–301

Contents lists available at SciVerse ScienceDirect

Atmospheric Research

journal homepage: www.elsevier.com/locate/atmos

Analysis of the columnar radiative properties retrieved during African desert dust events over Granada (2005–2010) using principal plane sky radiances and spheroids retrieval procedure

A. Valenzuela [a,b,*], F.J. Olmo [a,b], H. Lyamani [a,b], M. Antón [a,b], A. Quirantes [a], L. Alados-Arboledas [a,b]

[a] Departamento de Física Aplicada, Universidad de Granada, Fuentenueva s/n, 18071 Granada, Spain
[b] Centro Andaluz de Medio Ambiente (CEAMA), Av. del Mediterráneo s/n, 18006 Granada, Spain

ARTICLE INFO

Article history:
Received 7 July 2011
Received in revised form 11 November 2011
Accepted 11 November 2011

Keywords:
Mineral particles
Dust properties
Principal plane
Non-spherical particles

ABSTRACT

The southern Iberian Peninsula is an important area for studying the columnar radiative properties of African desert dust air masses reaching Europe. The Aerosol Optical Depth (AOD) and Angström coefficient, α (440–1020 nm), have been retrieved during the dust events reached at surface from 2005 to 2010 at Granada (37.18°N, 3.58°W, 680 m a.m.s.l), using extinction measurements by means of a CIMEL CE 318-1 sun-photometer. In addition, sky radiance measurements performed in principal plane in conjunction with solar irradiance measurements were used to retrieve columnar aerosol size distributions, single scattering albedo and asymmetry parameter. During these desert dust intrusions, high values of AOD at 440 nm (0.27 ± 0.17) and low values of α (0.4 ± 0.2) were found. These values indicate both high aerosol load and predominance of coarse particles during these events. The aerosol volume size distributions were bimodal, with the fine and coarse radius mode centered at 0.20 μm and 2.41 μm, respectively. The mean coarse to fine volume concentration ratio value was 11 ± 6, showing a predominance of coarse particles in good agreement with α analysis. During these events, columnar aerosol single scattering albedo (ω_0) increased with wavelength in accordance with previous works. However, the obtained values of ω_0 in all wavelengths were lower than those reported by other authors during desert dust intrusions. The mixing of desert dust with absorbing particles from anthropogenic origin could explain the low ω_0 values measured in the study area.

1. Introduction

Dust particles interact with the solar and thermal radiation modulating Earth's radiative budget. The Sahara desert is the most important source of mineral dust in Europe (Liu et al., 2008). North African desert dust is injected into the atmosphere through resuspension processes at the source areas, and it is then transported at different altitudes (from sea level up to 4–6 km) to different areas in the world (Escudero et al., 2005, 2011; Pavese et al., 2009). Mineral dust is responsible for approximately one third of global aerosol optical depth (Tegen et al., 1997), and absorbs solar radiation especially in the blue and ultraviolet wavelengths due to iron oxide impurities (Sokolik and Toon, 1999). It has been shown that the attenuation of solar radiation associated with dust particles is sensitive to their source region and the chemical and physical processes occurring during the transport of the dust. The Iberian Peninsula is frequently affected by African dust intrusion episodes with large aerosol load that can modulate the aerosol climatology in different areas of this region, particularly in the South.

Analyses of laboratory measurements and in situ data using scanning electron microscopes reveal that the shapes of dust particles are exclusively irregular (Koren et al., 2001;

* Corresponding author at: Centro Andaluz de Medio Ambiente, Av. del Mediterráneo s/n, 18006 Granada, Spain.
E-mail address: avalenzuela@ugr.es (A. Valenzuela).

0169-8095/$ – see front matter © 2011 Elsevier B.V. All rights reserved.
doi:10.1016/j.atmosres.2011.11.005

Muñoz et al., 2001). However, a common modeling practice in radiative transfer simulations and remote sensing implementations is to assume that dust particles are homogeneous spheres so that the classical Lorentz-Mie theory can be used. Mishchenko et al. (1997) showed that non-spherical such as dust particles produce angular scattering patterns different from area-equivalent spheres. Retrievals of the scattering phase function, especially at scattering angles larger than 90°, are important since this angular range determines the aerosol effect on climate and is used for remote sensing. Particle shape affects aerosol scattering at large scattering angles 100–140° (Dubovik et al., 2002; Olmo et al., 2006). The backscattering by non-spherical particles is usually less dependent on the scattering angle than by for spherical particles (Dubovik et al., 2002; Olmo et al., 2006). The difference between non-spherical and spherical scattering reaches a maximum value at scattering angle of 120° (Volten et al., 2001). Thus, it is convenient to include non-sphericity features for improving the retrieval qualities in particular for large dust particles. Numerous works have derived radiative properties of desert dust from measurements of sky radiance in the almucantar configuration (e.g., Dubovik et al., 2002; Kubilay et al., 2003; Lyamani et al., 2005; Tafuro et al., 2006; Olmo et al., 2006; Toledano et al., 2007a, 2007b; Cachorro et al., 2008; Pinker et al., 2010; Eck et al., 2010; Garcia et al., 2011; El-Metwally et al., 2011). However, few authors have used the sky radiance in the principal plane configuration (e.g. Olmo et al., 2008; Valenzuela et al., 2011). For instance, Olmo et al. (2008) analyzed the columnar aerosol radiative properties in Granada (Spain) using sky radiance in both configurations almucantar and principal plane. The aerosol properties obtained using these two configurations showed a good agreement for different African desert dust events.

Using the almucantar sky-radiance data the authors show that single scattering albedo can be retrieved with reasonably high accuracy only for high aerosol loading and large solar zenith angles (>50°), with accuracy to the level of 0.03 (Dubovik et al., 2002; Kim et al., 2004). But the aerosol load can change along the day also due to the different local sources or meteorological conditions. For low solar zenith angles the principal plane observations can be used instead of almucantar measurements (Dubovik et al., 2000; Olmo et al., 2008). The principal plane configuration measurements have identical capabilities as the almucantar configuration, but the advantage of the principal plane configuration is that you can reach scattering angles (sky radiance measurements) greater than 90° along the day, not just for large solar zenith angles, and would close the gap between morning and afternoon almucantar measurements. Measurements for scattering angles greater 90° are important to analyze the back-scattering properties in inversion schemes that include accurate radiative transfer models (Dubovik et al., 2000; Olmo et al., 2008). Thus, principal plane measurements and columnar aerosol optical properties derived from this configuration may be used to validate aerosol information retrieved from satellite sensors (e.g. MISR and POLDER) due to the relatively small solar zenith angles corresponding to their overpass time. The measurements from MISR and POLDER sensors present the advantage of multi-directionality with respect to one-directional MODIS observations, and thus they are considered as the basic data sets for joint inversions (Sinyuk et al., 2007). Therefore, inversion techniques using the principal plane configuration will play an outstanding role in the near future.

This paper focuses on the analysis of the columnar aerosol radiative properties retrieved during African desert dust air masses intrusions in Southern Iberian Peninsula from 2005 to 2010. In this paper we only consider events that reached the surface and were confirmed by CALIMA network (www.calima.ws) and sun-photometric measurements. Columnar radiative properties have been computed using the extinction measurements and sky radiance in the principal plane configuration by means of a non-spherical inversion code (Olmo et al., 2008). Therefore, this work will contribute to improve the understanding of the columnar radiative properties of African desert dust air masses far from the dust sources.

2. Experimental site and instrumentation

Measurements have been performed in the urban area of Granada, on the roof of the Andalucian Environmental Center — CEAMA (37.18°N, 3.58°W and 680 m a.m.s.l.). Granada, located in south-eastern Spain, is a non-industrialized, medium-sized city with a population of 300 000. The city is situated in a natural basin surrounded by mountains with altitudes over 1000 m. The near-continental conditions prevailing at this site are responsible for large seasonal temperature differences, providing cool winters and hot summers. The study area is also about 200 km away from the African continent, and approximately 50 km away from the western Mediterranean basin. Due to its proximity to the African continent our study area is frequently affected by Saharan dust intrusions (Lyamani et al., 2006a; Olmo et al., 2006, 2008).

Column-integrated characterization of the atmospheric aerosol has been performed by means of a sun-photometer CIMEL CE-318-4 included in the AERONET network (Holben et al., 1998). This sun-photometer makes direct sun measurements with a 1.2° full field of view at 340, 380, 440, 670, 870, 940 and 1020 nm. The full-width at half-maximum of the interference filters are 2 nm at 340 nm, 4 nm at 380 nm and 10 nm at all other wavelengths. In addition, the CIMEL instrument performs sky radiances, both in almucantar and principal plane, at 440, 670, 870 and 1020 nm. Calibration of this instrument was performed annually by AERONET-RIMA network. More details about CIMEL CE-318-4 can be found in Holben et al. (1998).

3. Methodology

The intrusions of the African desert dust air masses over the study area for the period 2005–2010 were identified using the information provided by the CALIMA network (www.calima.ws). The procedure of this network can be summarized in the following tasks: the CALIMA network produces periodically reports on the 24 h forecasts of dust outbreaks (e-mail alerts sent to air quality networks 24 h in advance). Later, using also information on the PM10 levels recorded at regional background stations in Spain, the CALIMA network produces a report of validations taking into account the different Spanish areas. To produce these reports the network uses HYSPLIT4 model (Draxler and Rolph, 2003; http://www.arl.noaa.gov/ready/hysplit4.html), synoptic meteorological charts

(http://www.ecmwf.int/), the maps of aerosol index of Ozone Monitoring Instrument (OMI) (ftp://toms.gsfc.nasa.gov/pub/omi/images/aerosol/), the SeaWiFS maps information (http://oceancolor.gsfc.nasa.gov/SeaWiFS/HTML/dust.htlm), the daily results of the aerosol models outputs such as SKIRON (http://forecast.uoa.gr), BSC-DREAM (http://www.bsc.es/projects/earthscience/DREAM/) and NAAPs (http://www.nrlmry.navy.mil/aerosol/), and, finally, the levels of PM10 recorded at regional background stations from air quality monitoring. In this sense, the reports of validated days correspond to African desert dust events tested by models, back-trajectory analysis, synoptic meteorological charts, satellite and surface data.

From the sun-photometer solar extinction measurements, the AOD at selected spectral channels and the Angström parameter (α) have been computed following the methods described in the works of Alados-Arboledas et al. (2003, 2008) and Estellés et al. (2006). All the measurement sequences are carried out following the AERONET protocols. The sun-photometer was calibrated by the AERONET team, and a linear rate change was assumed for the calibration coefficients. Pre- and post-field calibration, automatically cloud cleared and manually inspected were applied (similar procedure to AERONET level 2.0 AOD data).

The AOD (λ) was derived from the total optical depth retrieved from direct sun-photometer measurements data using the appropriate calibration constant and subtracting the Rayleigh optical depth, as well as the O_3 and NO_2. We compute Rayleigh, NO_2 and O_3 optical depth and optical air masses corresponding to the different constituents from the equations given by Gueymard (2001). To determine the total optical depth we employed the values of the extraterrestrial spectrum proposed by the SMARTS2 model (Gueymard, 2001), smoothing the data to the band pass of our sun-photometer. The NO_2 column contents were obtained from midlatitude model atmospheres in the LOWTRAN7 code (Kneizys et al., 1988). The O_3 column contents were taken from TOMS values (http:/toms.gsfc.nasa.gov).

The most important error in the calculation of the aerosol optical properties is the calibration uncertainties. The AOD (λ) absolute errors can be derived from Beer–Bouguer–Lambert law by error propagation theory (Reagan et al., 1986; Duran, 1997). As a result there are different uncertainty values for each wavelength depending on the processes involved. In our case, the combined effects result in a total uncertainty in AOD of about ± 0.01 for $\lambda > 440$ nm and ± 0.02 for shorter wavelengths, similar to AERONET level 2.0 data (Holben et al., 1998).

The error in α can be derived in a similar way, and considering α as a function of AOD at 440, 670, 870 and 1020 nm. The α errors are dependent on AOD errors and the inverse of the absolute value of AOD, and therefore dependent on the air mass: for low AOD values the error of α increases dramatically, even though the AOD accuracy is within specification (Toledano et al., 2007a, 2007b). In our case, taking into account the AOD and α values computed for the African desert dust air masses from 2005 to 2010, we expect α errors lower than 10%.

For the AOD (λ) retrieval we first remove cloud-contaminated measurements using the cloud screening method by Smirnov et al. (2000), which uses the difference of AOD (λ) between two consecutive measurements as a criterion determining the clear-sky condition. Even if data pass the threshold screening test, we only take data within three standard deviations from the mean in order to reduce uncertainties induced by cloud contamination (Smirnov et al., 2000; Alados-Arboledas et al., 2008).

The connection between the optical measurements and the columnar aerosol radiative properties occurs through the radiative transfer equation in a multiple-scattering scheme for a one-layer plane-parallel atmosphere. Nakajima et al. (1996) developed an inversion scheme for spherical particles that includes accurate radiative transfer modeling in order to account for multiple scattering effects. Olmo et al. (2006, 2008) adapted this methodology including shape mixtures of randomly oriented spheroids (equiprobable distributions of oblate and prolate) using the almucantar and principal plane measurement configurations. As input parameters the inversion procedures use the spectral AOD and the normalized spectral sky radiances in almucantar and principal plane configurations by means of a method that requires absolute calibration. As output parameters the code retrieves the effective columnar aerosol size distribution the phase function, the single scattering albedo and the asymmetry parameters. Detailed descriptions of the algorithm are found in Nakajima et al. (1996), Boi et al. (1999) and Olmo et al. (2006, 2008).

For the inversion retrievals the method uses the relative diffuse sky radiance (normalized by direct irradiance), $R(\Theta)$, that is less affected by deterioration of the interference filters of the sun-photometers, i.e.,

$$R(\Theta) = \beta(\Theta) + q(\Theta), \tag{1}$$

where $\beta(\Theta)$ is the total differential scattering coefficient, that is the sum of the scattering coefficients for aerosol and for molecules, and $q(\Theta)$ represents the contribution from multiple scattering.

In this method the aerosol optical depth, AOD (λ), is defined as

$$AOD(\lambda) = \frac{2\pi}{\lambda} \int_{r_{min}}^{r_{max}} k_{ext}(x,m) v(r) d\ln r, \tag{2}$$

where x is the size parameter, $v(r)(=\mathrm{dV/d\ ln\ r\ (cm^3\ cm^{-2})})$ is the columnar volume spectrum (aerosol size distribution), m is the complex refractive index, $K(x,m)$ is the kernel function, and r_{min} and r_{max} are minimum and maximum aerosol radii. The kernel function K_{ext} is defined as

$$K_{ext}(x,m) = \frac{3}{4} \frac{Q_{ext}(x)}{x}, \tag{3}$$

where Q_{ext} is the extinction efficiency. Also, in this method, the aerosol differential scattering coefficient is expressed as

$$\beta_A(\Theta) = \frac{2\pi}{\lambda} \int_{r_{min}}^{r_{max}} K(\Theta,x,m) v(r) d\ln r, \tag{4}$$

where K is the kernel function.

The algorithm retrieves the columnar size volume distributions from $\beta_A(\Theta)$ and AOD (λ) using an iterative inversion scheme. As the extinction coefficient can be expressed as the

sum of scattering and absorption coefficients, aerosol optical depth for the scattering can be obtained using Eq. (2) with the kernel function of scattering, and thus we can derive the monochromatic single scattering albedo (Kim et al., 2004).

The code uses the EBCM, or T-matrix, to calculate light scattering for non-spherical matrices (kernel matrices) instead of previously used Mie simulations by Nakajima (Nakajima et al., 1996). Accordingly, in code the aerosol single-scattering properties were defined as functions of the volume size distribution of randomly oriented polydisperse spheroids, and we computed the kernel matrices for randomly oriented prolate and oblate spheroids with aspect ratios ranging from 0.6 to 1.66, using equiprobable distributions, following the recommendations of Dubovik et al. (2002).

For the complex refractive index the selected value is invariant with wavelength. The optimal (effective) output parameters is retrieved by iteration and are that which minimize the residuals between measured and simulated normalized radiances. If the residuals are ≥10% the computation is discarded. The equation of the residuals used is as follows:

$$\Delta = \sqrt{\frac{\sum_{\lambda,\Theta}[(R_{\lambda\Theta} - C_{\lambda\Theta})/R_{\lambda\Theta}]}{N_\lambda N_\Theta}} \quad (5)$$

where R is the measured and C the calculated normalized sky radiance, and N is the number of wavelengths and scattering angles measured. λ and Θ refer to the wavelength and the scattering angle, respectively. All the available scattering angles in the range measured were used to retrieve the aerosol volume distribution in the radius interval 0.06–10 μm. The refractive indices used in the iterative process are: 1.33–1.55 (0.02 step) and 0–0.01 (0.0005 step) for the real part and imaginary part, respectively. The algorithm retrieves first the real part of the refractive index – assuming the imaginary part as zero – and then, fixing the real part, the imaginary part is retrieved. As the most favorable value for the surface albedo we select a constant value of 0.15 for Granada (Olmo et al., 2008).

Different studies show that the error of the retrieved columnar volume size distributions following these methodologies changes as a nonlinear function of particle size, aerosol type, and actual values of the size distribution (Boi et al., 1999; Dubovik et al., 2002). In particular, for the intermediate particle size range ($0.1 \leq r \leq 7$ μm) the retrieval errors do not exceed 10%, and may increase drastically up to about 35% for $r < 0.1$ μm and $r > 7$ μm because of the low sensitivity of the aerosol scattering at 440, 670, 870 and 1020 nm to particles of these sizes. These high errors in these ranges of r do not significantly affect the derivation of the main features of the columnar volume size distributions (Dubovik et al., 2002). On the other hand, the authors also show that the accuracy of single scattering albedo retrievals for high aerosol loading and sky radiance measurements including scattering angles close to 100° or greater is about 0.03, and the errors in complex refractive index are on the order of 30–50% for the imaginary part and 0.04 for the real part (Dubovik et al., 2000, 2002). Finally, the minimum value of the residuals given by the fit of the measured sky radiances to the computed sky radiances (Eq. (5)) is sensitive to both the presence of experimental error and the failure on the radiative model (inversion code). As the limit for the computed residuals is ≤10%, this residual value can be adopted as an indicator of the quality of the retrieval. The columnar effective parameters computed are not independent in the sense that the inversion code insures only the fact that the retrieved combination of all of these parameters would accurately reproduce the measured radiation field in the scope of the chosen radiative transfer model. Thus, the retrieval accuracy of each individual aerosol radiative parameter is dependent on the accuracy of the radiative transfer model.

In previous work the authors compared the results with the non-spherical method used in AERONET network — almucantar configuration (Olmo et al., 2006). The analyzed cases correspond to different atmospheric conditions and air masses origin over Granada, including conditions influenced by African desert dust air masses. For the inversion code using the almucantar configuration the results showed similar columnar phase functions, single scattering albedo, asymmetry parameter and size distributions for the micrometric mode, showing values with RMSD close to 1–7%. Also, the spectral dependence of the single scattering albedo and the asymmetry parameter were also comparable in both almucantar inversion methods. On the other hand, the authors showed the retrieval improvements of the method using the principal plane configuration (feasibility of extending the retrieval columnar radiative properties along the day) in different African desert dust air masses intrusions over Granada, and also the agreement of the two methods – almucantar and principal plane configurations – for the analyzed African desert dust events (Olmo et al., 2008).

Using the inversion code of Olmo et al. (2008) and sky radiance measurements in principal plane configuration, we computed a large set of columnar aerosol radiative parameters in the wavelengths 440, 670, 870 and 1020 nm during the African dust events that occurred from 2005 to 2010. The retrieved aerosol radiative properties include volume size distribution, single scattering albedo, $\omega_0(\lambda)$, and asymmetry parameter, g (λ). From the retrieved volume aerosol size distributions the effective radius and the mean modal radius as well as the volume concentration for total, fine and coarse modes were derived following the procedure of Dubovik et al. (2002). The cutoff radius used in size distributions for fine and coarse modes was 0.5 μm.

4. Results

CALIMA project reported 626 days affected by African desert dust air masses over the southern Iberian Peninsula from January 2005 to December 2010 (www.calima.ws): 78, 93, 139, 107, 115 and 94 days in 2005, 2006, 2007, 2008, 2009 and 2010, respectively. During the entire period 29% of days were characterized by the presence of African desert dust air masses, including events associated with cloudy conditions. The African dust intrusions were more frequent in summer (Jun, July and August) with a 45% of occurrence and less frequent in winter (11%). The numbers of days affected by these African desert dust air masses with sun-photometer cloud-free measurements were 12, 31, 25, 37, 33 and 45 for 2005, 2006, 2007, 2008, 2009 and 2010, respectively. This means a percentage of 9% for period 2005–2010. Toledano et al. (2007a) at El Arenosillo (Southwest Spain) from 2000 to 2004 reported that between 14% and 21% of days were

Table 1
Statistical parameters of AOD (440 nm), α (440–1020 nm) during desert dust events for the period 2005–2010, including: the mean, the standard deviation, the median, the first and the second quartile (P25 and P75).

		AOD_{1020}	AOD_{870}	AOD_{670}	AOD_{440}	$\alpha_{440-1020}$
No. of days with desert dust	183					
No. of observations	8680					
Mean		0.20	0.21	0.22	0.27	0.42
STD		0.13	0.14	0.14	0.15	0.21
Median		0.17	0.18	0.19	0.24	0.40
P25		0.11	0.25	0.28	0.17	0.26
P75		0.25	0.11	0.13	0.33	0.56

affected by desert dust intrusions. The large difference with our percentage of African desert dust events at Granada is due to the difference in detection method, considering only desert dust air masses detected at surface in our paper.

The statistics of the AOD and α during the African desert dust events recorded at Granada from 2005 to 2010 are summarized in Table 1. The mean value (±one standard deviation) of AOD (440 nm) (as reference wavelength for turbidity) was 0.27 ± 0.15. The large AOD standard deviation indicates a large variability in the atmospheric aerosol load during desert dust events. In this direction, the coefficient of variation (CV), defined as the ratio of the inter-quartile range (difference between the 75th and 25th percentile) to the median, also presents an elevated value (between 67% at 440 nm and 82% at 1020 nm). This large variation could be related to several factors such as different meteorological conditions, source region and the chemical and physical processes occurring during dust transport. Additional information on aerosol properties over the study area can be obtained from the analysis of the Angström parameter, α (440–1020 nm). The CV of this parameter presents a high value (75%) which indicates the presence of particles with different size during African dust episodes at Granada. Nevertheless, its mean value was small (0.4 ± 0.2), suggesting a significant contribution of coarse particles during these dust events.

The values of the AOD and α during African dust events obtained in Granada are in good agreement with those reported by Lyamani et al. (2005) during Sahara dust outbreak in the same study site. These authors, using sun-photometer data, have reported values of AOD (500 nm) ranging from 0.20 to 0.6 and values of α in the range 0.36–0.37. In addition, there is a good agreement with the data recorded on other AERONET sites influenced by desert dust. For example, Prats et al. (2008) reported mean values of AOD (440 nm) and α (440–870) of 0.40 ± 0.23 and 0.45 ± 0.26, respectively, at El Arenosillo during desert events. At this same location, Toledano et al. (2007a) have obtained during desert dust events a mean AOD (440 nm) value of 0.33 and a mean α value of 0.52.

Fig. 1 shows the frequency histograms of the AOD (440 nm) and α. Up to 35% of the AOD values were below 0.2. The principal frequency mode was centered at 0.24. Up to 7% of the AOD values were above 0.5. Two well-defined modes are observed in the histogram of α parameter. The principal frequency mode of α was centered at 0.4 and second mode was centered at 0.2. In addition, we also find mean values of α around 0.9. This situation could be related to the background conditions in this urban location, and also with the advection of air masses coming from Atlantic, Europe or the Mediterranean area, that leads to the simultaneous presence of desert dust with polluted aerosol in the atmospheric column. Toledano et al. (2007a, 2007b) have found at Arenosillo two main frequency modes of α. First the mode around 0.5 was related to the desert dust events, when the AOD increased and α decreased down to 0.2–0.4. On the other hand, the main frequency mode around 1.2 was related to the background conditions, that is, the mixture of marine aerosol with continental or urban-polluted aerosol. Prats et al. (2008) have shown a low alpha-mode centered ~0.4 at Arenosillo in summer 2004 which was associated with desert dust aerosol and marine background.

Fig. 2 shows a box diagram of the seasonal variability of AOD (440 nm) and α during the African dust events analyzed. In these box diagrams, the mean is represented by a blank dot and the median by a middle line. The top/bottom box limits represent the monthly mean plus/minus the standard deviation. In addition, the error bars of the box are the percentiles 5% and 95%. The number of data recorded during the months of January, November and December is quite limited due to

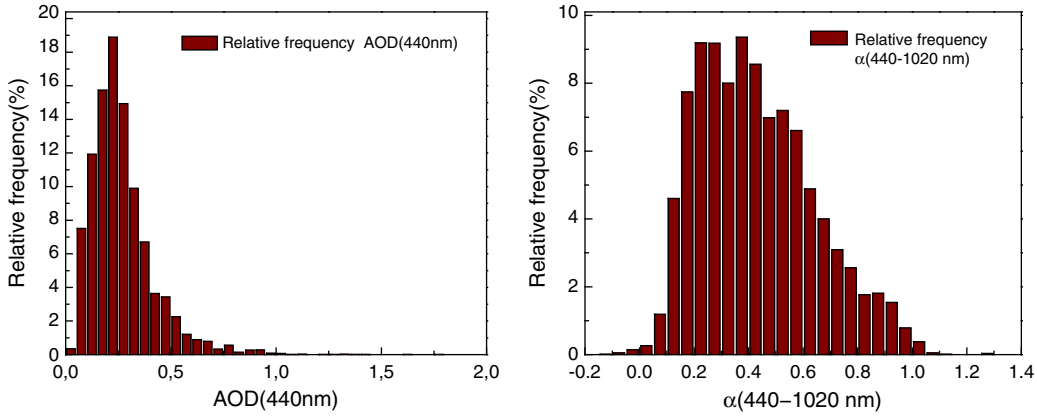

Fig. 1. Frequency histograms of AOD (440 nm) and α (440–1020 nm) (right plot) during African dust events for 2005–2010 period.

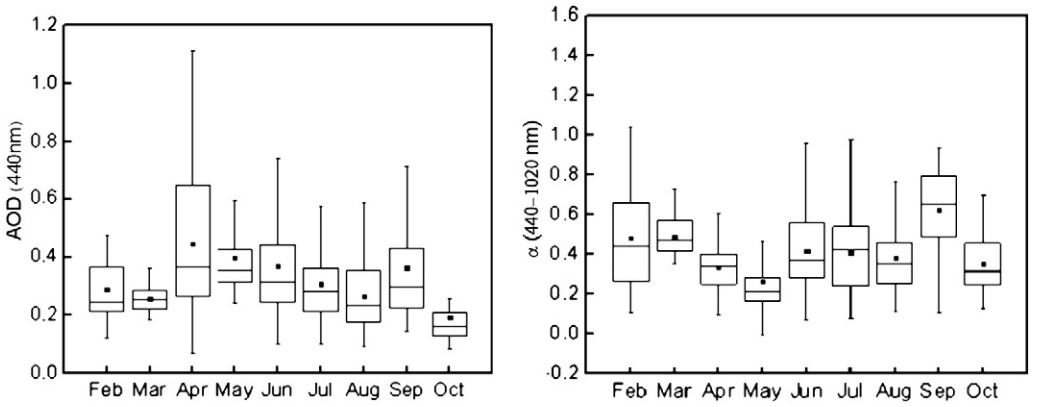

Fig. 2. Monthly statistics of AOD (440 nm) (left plot) and α (440–1020 nm) (right plot) during African dust events from 2005 to 2010 represented as box diagrams. In these box diagrams, the mean is represented by a blank dot and the median by a middle line. The top/bottom box limits represent the monthly mean plus/minus the standard deviation. In addition, the error bars of the box are the percentiles 5% and 95%.

the major presence of cloudy days. Fig. 2 (left plot) shows maximum monthly mean values of AOD (440 nm) in April (0.44 ± 0.24), and minimum values in October (0.19 ± 0.10). The spring and early summer months showed AOD values above 0.3 with a large variability for April. It is interesting to note that for almost all months the AOD mean values were higher than the median values, thus indicating the importance of scenarios with high aerosol load. Fig. 2 (right plot) shows that α varied in the range 0–1. The minimum mean values of α (440–1020 nm) were registered in May (0.27 ± 0.16), while the highest monthly mean value of this parameter was reached in September, with a mean value of 0.63 ± 0.21. The clear anti-correlation between aerosol optical depth and the Angström exponent, together with the reduced value of this last variable is an evident signature of the large contribution of coarse particles to the atmospheric aerosol during African desert dust episodes, in agreement with the observations reported by different authors (e.g. Smirnov et al., 1998; Cachorro et al., 2008; Toledano et al., 2007a; El-Askary et al., 2009; Eck et al., 2010). Nevertheless, the large error bars in both plots indicate significant variability in the aerosol load and particle size distribution at Granada during African dust events.

Table 2 summarizes the annual means of parameters related to columnar aerosol volume size distribution at Granada during desert dust events from 2005 to 2010. The parameters r_c and r_f are the modal radius for coarse and fine particles modes, respectively, and V_c and V_f are their volume concentrations. The cutoff radius used in size distributions for fine and coarse modes is 0.5 μm. The fine mode volume concentration, V_f, showed little changes during desert dust events with a mean value of 0.015 ± 0.007 $\mu m^3/\mu m^2$. The fine modal radius presents a mean value for the entire period close to 0.20 ± 0.04 μm. The fine mode aerosol showed no significant variation over the annual cycle in Granada which may be related mainly to the influence of the city: heavy traffic in the rather narrow streets together with the re-suspension of material available on the ground (e.g. Lyamani et al., 2006b, 2010).

The coarse mode volume concentration, V_c, showed a mean value of 0.17 ± 0.12 $\mu m^3/\mu m^2$ for the entire period, experiencing a notable seasonal change with the highest mean value in April (0.4 ± 0.4 $\mu m^3/\mu m^2$). In addition, the coarse modal radius showed a decreasing trend in February and March. The lowest mean value corresponded to March, 1.5 ± 0.3 μm, while the highest mean value corresponded to September (3.0 ± 1.6 μm). The coarse mode observed at Granada may be the result of a combination of different processes and source regions such as surface generated or transported dust particles from African desert regions.

The ratio V_c/V_f, 11 ± 6, indicated the prevalence of large particles with respect to small particles, which is characteristic of desert dust events. This ratio showed maximum mean

Table 2
Monthly and annual mean values of parameters related to aerosol volume size distribution at Granada during African dust events for 2005–2010 period.

	Coarse mode		Fine mode		V_c/V_f
	V_c ($\mu m^3/\mu m^2$)	r_c (μm)	V_f ($\mu m^3/\mu m^2$)	r_f (μm)	
February	0.14 ± 0.10	1.98 ± 1.18	0.016 ± 0.006	0.22 ± 0.03	8 ± 3
March	0.09 ± 0.03	1.46 ± 0.33	0.015 ± 0.003	0.20 ± 0.03	6 ± 2
April	0.42 ± 0.36	2.24 ± 1.27	0.031 ± 0.019	0.21 ± 0.05	14 ± 7
May	0.15 ± 0.12	2.29 ± 1.25	0.016 ± 0.005	0.20 ± 0.03	9 ± 6
June	0.16 ± 0.09	2.35 ± 1.39	0.015 ± 0.007	0.21 ± 0.04	10 ± 6
July	0.18 ± 0.09	2.47 ± 1.33	0.015 ± 0.005	0.20 ± 0.04	12 ± 5
August	0.14 ± 0.07	2.62 ± 1.43	0.012 ± 0.005	0.20 ± 0.03	12 ± 6
September	0.16 ± 0.09	3.01 ± 1.62	0.017 ± 0.008	0.19 ± 0.03	11 ± 7
October	0.12 ± 0.09	2.34 ± 1.46	0.012 ± 0.004	0.20 ± 0.04	10 ± 5
Annual	0.17 ± 0.12	2.41 ± 1.38	0.015 ± 0.007	0.20 ± 0.04	11 ± 6

values in April and minimum mean values in February and March, in concordance with the annual evolution of the Angström exponent.

For volume concentrations, Toledano et al. (2007b) found at El Arenosillo a mean V_c value of 0.11 $\mu m^3/\mu m^2$ lower than the value reported in this work for Granada (0.17 $\mu m^3/\mu m^2$). In contrast, the mean V_f value given by Toledano et al. (2007b) (0.023 $\mu m^3/\mu m^2$) for El Arenosillo was significantly higher than the value showed here (0.015 $\mu m^3/\mu m^2$). Prats et al. (2008), during desert dust event at El Arenosillo, showed an increase by a factor from up to 20 in the volume concentration of the coarse mode with respect to the fine mode. The differences respect to our results may be due to three reasons: a) differences related to the different measurement period (there is an inter-annual variability in the desert dust intrusions), b) differences related to the different of the desert dust intrusions detection method, and c) different pathways of the desert dust air masses during the transport until the two stations. These authors found mean values of 1.74 ± 0.15 μm for r_c and 0.13 ± 0.02 μm for r_f. These values are smaller than those obtained in the present work. On the other hand, Tafuro et al. (2006) found an averaged value of 2.2 μm for r_c, and an averaged value close to 15 for the ratio V_c/V_f at Lampedusa. This radiometric station is located 200 km away for northwest coast of Africa, approximately. Differences in dust amounts, anthropogenic or biomass burning contributions and air mass trajectories arriving at Lampedusa must be responsible for the differences with respect to our study. On the other hand, the volume concentration and the modal radius of coarse particles obtained in our study have higher standard deviations, which is indicative of the wide dust particles variability with different optical and microphysical properties. The standard deviations for modal radius of fine particles present small values, close to ± 0.03 μm, showing the lower variability of particles size with anthropogenic or biomass burning origin. Finally, Table 2 shows that the fine mode parameters present no significant change whereas the coarse mode parameters were a good indicator of the dust desert arrival. These values were consistent with those obtained by other authors for desert dust events (e.g., Olmo et al., 2006, 2008; Dubovik et al., 2002; Toledano et al., 2007a; Lyamani et al., 2006a).

Both single scattering albedo (ω_0) and asymmetry parameter (g) are key parameters for estimating the direct radiative impact of aerosol particles. The ω_0 is defined as the ratio of the scattering coefficient and the extinction coefficient, and it is related to the absorptive capacity of the aerosol, taking a value of 1 for pure scattering particles and below 1 for absorbing ones. Absorption of solar radiation by atmospheric particles results mainly from elemental carbon originated from anthropogenic activities, biomass burning and mineral dust. According to the literature, the ω_0 varies between 0.78 and 0.94 for cases of biomass burning particles and between 0.92 and 0.99 when the dominant particles are of desert type (Dubovik et al., 2002). Particularly, g provides information of the angular distribution of the scattered radiation. For hemispherically symmetric scattering, Rayleigh scattering, the asymmetry parameter is considered to be 0 and for pure forward scattering g would be 1.

In the analyzed period, mean values of ω_0 ranged from 0.89 ± 0.02 at 440 nm to 0.92 ± 0.03 at 1020 nm. These results are in a good agreement with the results obtained during the dust outbreaks by Lyamani et al. (2006a) and Olmo et al. (2006) in the same study area. Perrone et al. (2005) also showed similar results at Lecce (Italy) with values of ω_0 (440 nm) ranging from 0.85 to 0.9 when their study area was affected by Saharan dust together with anthropogenic aerosols from the central Mediterranean. However, the values of ω_0 reported in this work were lower than those reported by other authors for cases of pure desert dust. Dubovik et al. (2002) at Cape Verde obtained an averaged ω_0 value at 440 nm of 0.93. Kim et al. (2011) found in Tamanraset (in 2006–2009 period) that ω_0 ranging from 0.90 to 0.94 at 440 nm during desert dust events. The columnar values retrieved at Granada include the urban contribution that could be responsible of lower ω_0 values (Lyamani et al., 2006b, 2010). On the other hand, the long-range transport and the possible mixing with different aerosol types from source regions could be another reason for the lower ω_0 values (Lyamani et al., 2006b; Lyamani et al., 2010; Gomez-Amo et al., 2011). Close to the source region mostly pure dust is found, but after a long range transport the aging of the dust and mixing with other aerosol types modify the optical properties of the desert dust (Bauer et al., 2011). The mixing of desert dust with anthropogenic particles may prompt changes in the physical properties and chemical composition of the desert dust and this may have important consequences in processes affecting climate (Rodrıguez et al., 2011). The low values of ω_0 obtained in our study area reveal the importance of aerosol absorption during desert dust events at Granada.

Fig. 3 shows the annual evolution of monthly mean ω_0 for 440, 670, 870 and 1020 nm from 2005 to 2010. The most important feature of ω_0 was its spectral variation (slight increase with wavelength) as shown in other studies for desert dust events (e.g., Collaud Coen et al., 2004; Lyamani et al., 2006b; Alados-Arboledas et al., 2008; Cachorro et al., 2008; Su and Toon, 2011; Toledano et al., 2011; El-Metwally et al., 2011). In addition, it can be seen that the highest monthly mean value was found in February with ω_0 ranging from 0.94 ± 0.02 (at 440 nm) to 0.96 ± 0.03 (at 1020 nm), respectively. For spring and summer months the monthly mean values increased with wavelength. Mean values of ω_0 for July ranged from 0.88 ± 0.02 to 0.91 ± 0.03 at 440 and 1020 nm, respectively. This last fact is characteristic of mineral dust (Eck et al., 2010). Additionally, Fig. 3 also shows a decreasing

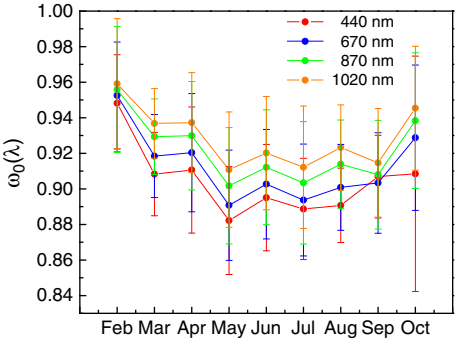

Fig. 3. Monthly mean values of ω_0 (λ) for 440, 670, 870 and 1020 nm during African dust events from 2005 to 2010, and standard deviation values.

of ω_0 at all wavelengths in spring and summer seasons, indicating a higher contribution of absorbing particles at Granada, probably due to the anthropogenic or biomass burning contributions associated with the synoptic situations of these months (Lyamani et al., 2005; 2006b; 2010).The difference between ω_0 (440 nm) and ω_0 (1020 nm) shows higher values in spring (March, April and May) and summer (Jun, July and August) than in February and October. The ω_0 values show strongly wavelength dependence during spring and summer and relatively lesser dependence in February and October. This fact could be related to a larger influence of absorbing aerosol during warm-seasons. Kim et al. (2011) show in Tamanraset (in the center of the Saharan desert) that in the months between March and September there are more dusty days. However, they found in the annual evolution of the single scattering albedo lower values in the months from May to August ($\omega_0 = 0.90 \pm 0.02$ at 440 nm).This result is similar to the annual evolution of the single scattering albedo during desert dust events in our site from 2005 to 2010 period.

The asymmetry parameter, g, showed distinct wavelength dependence with mean values ranging from 0.70 ± 0.02 at 440 nm to 0.67 ± 0.02 at 1020 nm. Our results confirm the values derived by Olmo et al. (2006) with 0.69 ± 0.02 at 440 nm to 0.66 ± 0.02 at 1020 nm during Saharan dust episodes in the same study area. Dubovik et al. (2002), for desert dust episodes, have obtained values of g (440 nm) around 0.69 ± 0.04 at Solar Ville, Saudi Arabia, and around 0.73 ± 0.04 at Cape Verde in these same wavelengths.

Fig. 4 shows the monthly mean values of g at 440, 670, 870 and 1020 nm. The g values showed no significant seasonal and spectral variation for the four wavelengths. This behavior is characteristic of mineral dust (e.g. Alados-Arboledas et al., 2008). Nevertheless, a slightly higher value for g (440 nm) values is observed. These differences agree with the results reported by Lyamani et al. (2006b) for the extreme desert dust event registered during the 2003 heat wave at Granada. Kim et al. (2011) show the annual evolution for g (λ) in several locations in African North (Tamanraset, Cape Verde, Solar Village and Banizoumbou). They compare this evolution of g (λ) for the entire data set and only in case of desert dust. The difference of g (λ) between the two is close to zero. In addition, similar to our study, g (λ) does not show significant differences between all months.

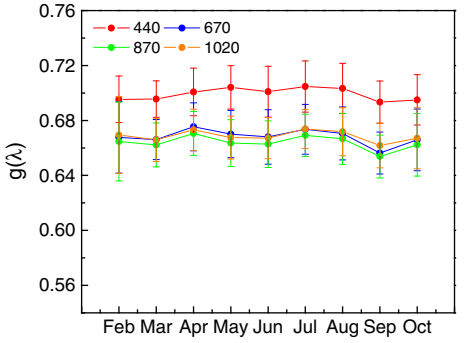

Fig. 4. Monthly mean values of g (λ) for 440, 670, 870 and 1020 nm during African dust events from 2005 to 2010, and standard deviation values.

5. Conclusions

In this paper we have analyzed the columnar aerosol radiative properties over Granada (Spain) during the African dust events occurring from 2005 to 2010. We used sun-photometric measurements (extinction and sky radiances) for cloudless days and only events confirmed by the CALIMA project with dust at the surface. The inversion code used includes non-spherical particles consideration and principal plane configuration for sky radiances.

The mean value of AOD (440 nm) was 0.27 ± 0.15. For the entire period a seasonal pattern was found, with two annual peaks in spring and early summer and September, and a clear decrease in October and February. The mean value of α was 0.42 ± 0.21 for the entire period. The high AOD values and low α values indicated the prevalence of coarse particles during desert dust events. The magnitude of the Angstrom exponent (α) presented low values throughout the year with the lowest ones in spring and summer.

The aerosol volume size distribution showed bimodal distribution, with the fine and coarse radius mode close to 0.20 ± 0.04 μm and 2.41 ± 1.38 μm, respectively. The most relevant result has been the high mean value of coarse mode volume concentration which is indicative of its outstanding contribution of dust particles. This mode was evidently dominant during the entire period due to the prevalence of dust particles with relatively large size, leading to a volume concentration ratio of coarse to fine modes of 11 ± 6.

The averaged values of ω_0 and g at the four wavelengths 440, 670, 870 and 1020 nm were 0.91 ± 0.03 and 0.68 ± 0.02, respectively. These values were consistent with those obtained by other authors in the same study area for desert dust events. However, ω_0 showed smaller values than those reported in the literature for pure desert dust. The mixing of desert dust with absorbing particles from anthropogenic origin (during all year) and biomass burning contribution (mainly in summer) could explain these low ω_0 values at the study area.

We would like to highlight that the desert dust events are a relevant factor for the estimation of the aerosol forcing impact in areas like southern Spain. In future works we will analyze the columnar aerosol radiative properties taking into account the origins and sectors of air mass trajectories and the associated synoptic conditions which favor the arrival of desert dust from North Africa for this period. Additionally, the aerosol forcing impact will be evaluated.

Acknowledgments

This work was supported by the Andalusia Regional Government through projects P08-RNM-3568 and P10-RNM-6299, by the Spanish Ministry of Science and Technology through projects CGL2008-01330-E/CLI (Spanish Lidar Network), CGL2010-18782 and CSD2007-00067; and by EU through ACTRIS project (EU INFRA-2010-1.1.16-262254). We acknowledge the NOAA Air Resources Laboratory (ARL) for the use of HYSPLIT model. We would like express their gratitude to the CALIMA project.

References

Alados-Arboledas, L., Lyamani, H., Olmo, F.J., 2003. Aerosol size properties at Armilla, Granada (Spain). Q. J. R. Meteorol. Soc. 129, 1395–1413.

Alados-Arboledas, L., Alcántara, A., Olmo, F.J., Martínez-Lozano, J.A., Estellés, V., Cachorro, V., Silva, A.M., Horvath, H., Gangl, M., Díaz, A., Pujadas, M., Lorente, J., Labajo, A., Sorribas, M., Pavese, G., 2008. Aerosol columnar properties retrieved from CIMEL radiometers during VELETA 2002. Atmos. Environ. 42, 2654–2667.

Bauer, S., Bierwirth, E., Esselborn, M., Petzold, A., Macke, A., Trautmann, T., Wendisch, M., 2011. Airborne spectral radiation measurements to derive solar radiative forcing of Saharan dust mixed with biomass burning smoke particles. Tellus 63B, 742–750.

Boi, P., Tonna, G., Dalu, G., Nakajima, T., Olivieri, B., Pompei, A., Campanelli, M., Rao, R., 1999. Calibration and data elaboration procedure for sky irradiance measurements. Appl. Opt. 38 (6), 896–907.

Cachorro, V.E., Toledano, C., Prats, N., Sorribas, M., Mogo, S., Berjón, A., Torres, B., Rodrigo, R., de la Rosa, J., De Frutos, A.M., 2008. The strongest desert dust intrusion mixed with smoke over the Iberian Peninsula registered with Sun photometry. J. Geophys. Res. 113, D14S04. doi:10.1029/2007JD009582.

Collaud Coen, M., Weingartner, E., Schaub, D., Hueglin, C., Corrigan, C., Henning, S., Schwikowski, M., Baltensperger, U., 2004. Saharan dust events at the Jungfraujoch: detection by wavelength dependence of the single scattering albedo and first climatology análisis. Atmos. Chem. Phys. 4, 1–16.

Draxler, R.R., Rolph, G.D., 2003. HYSPLIT (HYbrid Single-Particle Lagrangian Integrated Trajectory) Model. http://www.arl.noaa.gov/ready/hysplit4.html NOAA Air Resour. Lab., Silver Spring, MD.

Dubovik, O., Smirnov, A., Holben, B.N., King, M.D., Kaufman, Y.J., Eck, T.F., Slutsker, I., 2000. Accuracy assessment of aerosol optical properties retrieved from Aerosol Robotic Network (AERONET) sun and sky radiance measurements. J. Geophys. Res. 105, 9791–9806.

Dubovik, O., Holben, B., Eck, T.F., Smirnov, A., Kaufman, Y.J., King, M.D., Tanre, D., Slutsker, I., 2002. Variability of absorption and optical properties of key aerosol types observed in worldwide locations. J. Atmos. Sci. 59, 590–608.

Duran P. 1997. Medidas espectrorradiométricas para la determinación de componentes atmosféricos (ozono, vapor de agua y aerosoles) y modelización del intercambio radiativo en la atmósfera. PhD thesis, Universidad de Valladolid, Spain.

Eck, T.F., Holben, B.N., Sinyuk, A., Pinker, R.T., Goloub, P., Chen, H., Chatenet, B., Li, Z., Singh, R.P., Tripathi, S.N., Reid, J.S., Giles, D.M., Dubovik, O., O'Neill, N.T., Smirnov, A., Wang, P., Xia, X., 2010. Climatological aspects of the optical properties of fine/coarse mode aerosol mixtures. J. Geophys. Res. 115, D19205. doi:10.1029/2010JD014002.

El-Askary, H., Farouk, R., Ichoku, C., Kafatos, M., 2009. Transport of dust and anthropogenic aerosols across Alexandria, Egypt. Ann. Geophys. 27, 2869–2879.

El-Metwally, M., Alfaro, S.C., Abdel Wahab, M.M., Favez, O., Mohamed, Z., Chatenet, B., 2011. Aerosol properties and associated radiative effects over Cairo (Egypt). Atmos. Res. 99, 263–276.

Escudero, M., Castillo, S., Querol, X., Avila, A., Alarcón, M., Viana, M.M., Alastuey, A., Cuevas, E., Rodríguez, S., 2005. Wet and dry African dust episodes over eastern Spain. J. Geophys. Res. 110, 1–15.

Escudero, M., Stein, A.F., Draxler, R.R., Querol, X., Alastuey, A., Castillo, S., Avila, A., 2011. Source apportionment for African dust outbreaks over the Western Mediterranean using the HYSPLIT model. Atmos. Res. 99, 518–527.

Estellés, V., Utrillas, M.P., Martínez-Lozano, J.A., Alcántara, A., Alados-Arboledas, L., Olmo, F.J., Lorente, J., de Cabo, X., Cachorro, V., Horvath, H., Labajo, A., Sorribas, M., Díaz, J.P., Díaz, A.M., Silva, A.M., Elías, T., Pujadas, M., Rodrigues, J.A., Cañada, J., García, Y., 2006. Intercomparison of spectroradiometers and Sun photometers for the determination of the aerosol optical depth during the VELETA-2002 field campaign. J. Geophys. Res. 111, D17207. doi:10.1029/2005JD006047.

Garcia, O.E., Exposito, F.J., Diaz, J.P., Diaz, A.M., 2011. Radiative forcing under mixed aerosol conditions. J. Geophys. Res. 116, D01201. doi:10.1029/2009JD013625.

Gomez-Amo, J.L., Pinti, V., Di Iorio, T., di Sarra, A., Meloni, D., Becagli, S., Bellantone, V., Cacciani, M., Fua, D., Perrone, M.R., 2011. The June 2007 Saharan dust event in the central Mediterranean: observations and radiative effects in marine, urban, and sub-urban environments. Atmos. Environ. 45, 5385–5393.

Gueymard, C., 2001. Parameterized transmittance model for direct beam and circumsolar spectral irradiance. Solar Energy 71 (5), 325–346.

Holben, B.N., Eck, T.F., Slutsker, I., Tanre, D., Buis, J.P., Setzer, A., Vermote, E., Reagan, J.A., Kaufman, Y.J., Nakajima, T., Lavenu, F., Jankowiak, I., Smirnov, A., 1998. AERONET — a federated instrument network and data archive for aerosol characterization. Remote. Sens. Environ. 66, 1–16.

Kim, D.H., Sohn, B.J., Nakajima, T., Takamura, T., Takemura, T., Choi, B.C., Yoon, S.C., 2004. Aerosol optical properties over east Asia determined from ground-based sky radiation measurements. J. Geophys. Res. 109, D02209. doi:10.1029/2003JD003387.

Kim, D., Chin, M., Yu, H., Eck, T.F., Sinyuk, A., Smirnov, A., Holben, B.N., 2011. Dust optical properties over North Africa and Arabian Peninsula derived from the AERONET dataset. Atmos. Chem. Phys. Discuss. 11, 20181–20201.

Kneizys, F.X., Shettle, E.P., Abreu, L.W., Chetwind, J.H., Anderson, G.P., Gallery, W.O., et al., 1988. Users Guide to LOWTRAN7, Environmental Research Paper 1010. US Air Force Geophys. Lab, Bedford, MA.

Koren, I., Ganor, E., Joseph, J.H., 2001. On the relation between size and shape of desert dust aerosol. J. Geophys. Res. 106, 18047–18054.

Kubilay, N., Cokacar, T., Oguz, T., 2003. Optical properties of mineral dust outbreaks over the northeastern Mediterranean. J. Geophys. Res. 108 (D21), 4666. doi:10.1029/2003JD003798.

Liu, Z., Omar, A., Vaughan, M., Hair, J., Kittaka, C., Hu, Y., Powell, K., Trepte, C., Winker, D., Hostetler, C., Ferrare, R., Pierce, R., 2008. CALIPSO lidar observations of the optical properties of Saharan dust: a case study of long-range transport. J. Geophys. Res. 113, D07207. doi:10.1029/2007JD008878.

Lyamani, H., Olmo, F.J., Alados-Arboledas, L., 2005. Saharan dust outbreak over southeastern Spain as detected by sun photometer. Atmos. Environ. 39, 7276–7284.

Lyamani, H., Olmo, F.J., Alcántara, A., Alados-Arboledas, L., 2006a. Atmospheric aerosols during the 2003 heat wave in southeastern Spain I: spectral optical depth. Atmos. Environ. 40, 6453–6464.

Lyamani, H., Olmo, F.J., Alcántara, A., Alados-Arboledas, L., 2006b. Atmospheric aerosols during the 2003 heat wave in southeastern Spain II: microphysical columnar properties and radiative forcing. Atmos. Environ. 40, 6465–6476.

Lyamani, H., Olmo, F.J., Alados-Arboledas, L., 2010. Physical and optical properties of aerosols over an urban location in Spain: seasonal and diurnal variability. Atmos. Chem. Phys. 10, 239–254.

Mishchenko, M.I., Travis, L.D., Kahn, R.A., West, R.A., 1997. Modeling phase functions for dustlike tropospheric aerosols using a shape mixture of randomly oriented polydisperse spheroids. J. Geophys. Res. 102, 16831–16847.

Muñoz, O., Volten, H., de Haan, J.F., Vassen, W., Hovenier, J.W., 2001. Experimental determination of scattering matrices of randomly oriented fly ash and clay particles at 442 and 633 nm. J. Geophys. Res. 106, 22833–22844.

Nakajima, T., Tonna, G., Rao, R.Z., Boi, P., Kaufman, Y., Holben, B., 1996. Use of sky brightness measurements from ground for remote sensing of particulate polydispersions. Appl. Opt. 35, 2672–2686.

Olmo, F.J., Quirantes, A., Alcantara, A., Lyamani, H., Alados-Arboledas, L., 2006. Preliminary results of a non-spherical aerosol method for the retrieval of the atmospheric aerosol optical properties. J. Quant. Spectrosc. Radiat. Transfer 100, 305–314.

Olmo, F.J., Quirantes, A., Lara, V., Lyamani, H., Alados-Arboledas, L., 2008. Aerosol optical properties assessed by an inversion method using the solar principal plane for non-spherical particles. J. Quant. Spectrosc. Radiat. Transfer 109, 1504–1516.

Pavese, G., De Tomasi, F., Calvello, M., Esposito, F., Perrone, M.R., 2009. Detection of Sahara dust intrusions during mixed advection patterns over south-east Italy: a case study. Atmos. Res. 92, 489–504.

Perrone, M.R., Santese, M., Tafuro, A.M., Holben, B.N., Smirnov, A., 2005. Aerosol load characterization over southeast Italy for one year of AERONET sun-photometer measurements. Atmos. Res. 75, 111–133.

Pinker, R.T., Liu, H., Osborne, S.R., Akoshile, C., 2010. Radiative effects of aerosols in sub-Sahel Africa: dust and biomass burning. J. Geophys. Res. 115, D15205. doi:10.1029/2009JD013335.

Prats, N., Cachorro, V.E., Sorribas, M., Mogo, S., Berjon, A., Toledano, C., De Frutos, A.M., de la Rosa, J., Laulainen, N., de la Morena, B.A., 2008. Columnar aerosol optical properties during "El Arenosillo 2004 summer campaign". Atmos. Environ. 42, 2643–2653.

Reagan, J.A., Thomason, L.W., Herman, B.M., Palmer, J.M., 1986. Assessment of atmospheric limitations on the determination of the solar spectral constant from ground-based spectroradiometer measurements. IEEE Trans. Geosci. Remote Sens. GE-24, 258–265.

Rodrıguez, S., Alastuey, A., Alonso-Perez, S., Querol, X., Cuevas, E., Abreu-Afonso, J., Viana, M., Pandolfi, M., de la Rosa, J., 2011. Transport of desert dust mixed with North African industrial pollutants in the subtropical Saharan air layer. Atmos. Chem. Phys. 11, 6663–6685.

Sinyuk, A., Dubovik, O., Holben, B., Eck, T.F., Breon, F.M., Martonchik, J., Kahn, R., Diner, D.J., Vermote, E.F., Roger, J.C., Lapyonok, T., Slutsker, I., 2007. Simultaneous retrieval of aerosol and surface properties from a combination of AERONET and satellite data. Remote. Sens. Environ. 107, 90–108.

Smirnov, A., Holben, B.N., Slutsker, I., Welton, E.J., Formenti, P., 1998. Optical properties of Saharan dust during ACE 2. J. Geophys. Res. 103, 28079–28092.

Smirnov, A., Holben, B.N., Eck, T.F., Dubovik, O., Slutsker, I., 2000. Cloud-screening and quality control algorithms for the AERONET database. Remote. Sens. Environ. 73, 337–349.

Sokolik, I.N., Toon, O.B., 1999. Incorporation of mineralogical composition into models of the radiative properties of mineral aerosol from UV to IR wavelengths. J. Geophys. Res. 104, 9423–9444.

Su, L., Toon, O.B., 2011. Saharan and Asian dust: similarities and differences determined by CALIPSO, AERONET, and a coupled climate-aerosol microphysical model. Atmos. Chem. Phys. 11, 3263–3280.

Tafuro, A.M., Barnaba, F., De Tomasi, F., Perrone, M.R., Gobbi, G.P., 2006. Saharan dust particle properties over the central Mediterranean. Atmos. Res. 81, 67–93.

Tegen, I., Hollrig, P., Chin, M., Fung, I., Jacob, D., Penner, J., 1997. Contribution of different aerosol species to the global aerosol extinction optical thickness: estimates from model results. J. Geophys. Res. 102, 23895–23915.

Toledano, C., Cachorro, V.E., Berjon, A., de Frutos, A.M., Sorribas, M., de la Morena, B.A., Goloub, P., 2007a. Aerosol optical depth and Angstrom exponent climatology at El Arenosillo AERONET site (Huelva, Spain). J. Quant. Spectrosc. Radiat. Transfer 133, 795–807.

Toledano, C.V.E., de Cachorro, A.M., Frutos, M., Sorribas, N. Prats, de la Morena, B.A., 2007b. Inventory of African desert dust events over the southwestern Iberian Peninsula in 2000–2005 with an AERONET Cimel Sun photometer. J. Geophys. Res. 112, D21201. doi:10.1029/2006JD008307.

Toledano, C., Wiegner, M., Gross, S., Freudenthaler, V., Gasteiger, J., Mueller, D., Mueller, T., Schladitz, A., Weinzierl, B., Torres, B., O'Neill, N.T., 2011. Optical properties of aerosol mixtures derived from sun-sky radiometry during SAMUM-2. Tellus 63B, 635–648.

Valenzuela, A., Olmo, F.J., Lyamani, H., Quirantes, A., Alados-Arboledas, L., 2011. Aerosol radiative properties retrieved during Saharan dust events in Southeastern Spain from 2005 to 2008. Opt. Pura y Apl. 44 (4), 661–664.

Volten, H., Muñoz, O., Rol, E., de Haan, J.F., Vassen, W., Hovenier, J.W., 2001. Scattering matrices of mineral aerosol particles at 441.6 nm and 632.8 nm. J. Geophys. Res. 106 (D15), 17375–17401.